2013 IEEE/RSJ International Conference on
Intelligent Robots and Systems (IROS)
November 3-7, 2013. Tokyo, Japan

A CPG-based Locomotion Control Architecture for Hexapod Robot

Haitao Yu, Wei Guo, Jing Deng, Mantian Li and Hegao Cai

Abstract—**This paper proposes a novel CPG-based control architecture for hexapod walking robot. We investigate the CPG systems from the perspective of network synchronization. In this way the motion control of hexapod robot can be refined into the gait generation level and joints coordination level. On the first level, we develop a gait generator consists of CPG network in ring based on modified Van der Pol (VDP) oscillator to realize various stable gaits as well as gait transition for hexapod walking. The limit cycle behavior of VDP model is analytically studied by virtue of perturbation technique. On the second level, we address the problem of multi-DoF coordination of single leg via phase order modulation and amplitude adjustment of the neural oscillators. Consequently we propose a single-leg controller consists of a three-coupled CPG network and a linear coefficient converter to generator smooth and feasible trajectories in task space. The effectiveness of the proposed control architecture is demonstrated through simulation and real physical robot experiment.**

I. Introduction

The rhythmic and agile behavior displayed by legged animals when interact with irregular terrain outclasses any man-made robots at present. This robust and stable performance has been attracting the interest of scientists and engineers to develop analogous walking machines with environment adaptability such as Raibert's hoppers [1], Rhex [2], Tarry [3], Tekken [4] and Salamander [5]. Generally, this work is still in its infancy because the advancement of bio-inspired control awaits empirical evidence in anatomy and neurophysiology. Central pattern generators (CPGs), also known as a group of coupled nonlinear oscillators, are neural networks that generate self-adjusted rhythmic patterned signals without sensory feedback or higher-level command [6-8]. These unique characteristics of CPGs have been widely used in biologically inspired robots.

The concept of CPG has been successfully applied to bionic robots for nearly thirty years. The first CPG model (also named as neural rhythm generators), simple but effective, was proposed by Matsuoka in 1987 [9]. As a novel control technology since then, the CPG-based regulator to control the locomotion of robots had become a potential method to cope with multi-DoF motion control of legged robots. Taga *et al*. [10] realized stable CPG-controlled bipedal walking when negotiating obstacles. Kimura *et al*. [4] studied the motion control of quadruped robot based on CPG integrating sensory feedback. Manoonpong *et al*. [11] developed chaotic CPGs to control the hexapod robot with leg damage compensation. Crespi *et al*. [12], Ijspeert *et al*. [13] and Ma *et al*. [14] also regulated the swimming robot with CPG methods.

The traditional methods of developing CPG-based locomotion controller can be summarized as two steps. First, establish a neural network of coupled nonlinear oscillators which exert periodic signals via neuron interaction. Second, tune the parameters of the network in order to shape the outputs of CPG in accordance with the mechanical structure of the robot. Admittedly, it is still a challenge to determine the connection and coupling weights of the CPG network. Learning and optimization algorithms are applied to this issue as an alternative. Prentice *et al*. [15] proposed a gradient-descent learning approach to solve the parameter determination of the neuron network. Okada *et al*. [16] introduce the concept of vector fields learning and Ijspeert developed a statistical learning approach to study the nonlinear oscillator with adjustable frequency in [17]. Beer et al [18] designed the nonlinear coupled recurrent neuron network via evolutionary algorithm to suitable outputs for legged locomotion. Generally, these learning, optimization as well as evolutionary methods are time-consuming and compute-intensive work, which makes the algorithms difficult to transfer into the robot application domain.

The motivation of this work is to systematically construct CPG-based control architecture for hexapod locomotion so as to enhance the adaptation of legged robots with various gait types and achieve smooth gait transition. To solve the problems mentioned above, this paper presents a novel CPG-based control architecture for hexapod robot. The perturbation method is also applied to analytically investigate the limit cycle behavior of Van der Pol oscillator which is the basic element of CPG network. The gait generator together with the single-leg controller has been developed to achieve various stable gait and gait transition.

The reminder of the paper is structured as follows. In section II, the CPG model based on Van der Pol oscillator is introduced. The CPG-based locomotion controller for hexapod walking robot is presented in Section III. The hexapod robot prototype and test environment is described in Section IV, followed by the simulation and experiment results. This paper ends with conclusions and discussion in Section V.

II. CPG Model

This section presents the neuron model of CPG network, which consists of nonlinear oscillators to generate stable output signal for rhythmic regulation of hexapod locomotion. Based on the perturbation technique, the analytical description of the neuron model can be obtained. In this manner, the

This work is supported by National Hi-tech Research and Development Program of China (863 Program, Grant No. 2011AA040701), National Natural Science Foundation of China (No. 61175107, No. 61005076) and Self-Planned Task (No. SKLRS201006B, No. SKLRS201204B) of State Key Laboratory of Robotics and System (HIT)

Haitao Yu is with the Dept. of Mechanical Engineering, Harbin Institute of Technology, 150001 Harbin, China arcoyu@gmail.com

Wei Guo is with the Dept. of Mechanical Engineering, Harbin Institute of Technology, 150001 Harbin, China wwg65@yahoo.com.cn

Jing Deng, Mantian Li and Hegao Cai are with the State Key Laboratory of Robotics and System, Harbin Institute of Technology, 150080 Harbin, China {dengjing,limt, hgcai}@hit.edu.cn

parametrical analysis of CPG model can be systematically conducted.

A. Van der Pol Oscillator

The Van der Pol (VDP) oscillator has been widely used in both physical and biological research since proposed in [19]. Considering the tractability in mathematics and application to hexapod locomotion control, this paper presents a novel nonlinear oscillator model via modifying the coefficient of nonlinear quadratic term without loss the general dynamical properties of the original VDP model, namely, the limit cycle behavior. The single neuron model can be written as

$$\ddot{x} + \varepsilon(bx^2 - 1)\dot{x} + \omega_0^2 x = 0 \tag{1}$$

where x denotes the state variable of the VDP oscillator, ε represents the coefficient of nonlinear quadratic term, b and ω_0 represent the amplitude adjustment parameter and natural frequency of the affiliated linear vibration system of (1).

Rewriting the nonlinear differential equation (1) into state-space form, we have

$$\begin{cases} \dot{x} = y \\ \dot{y} = \varepsilon(1 - bx^2)y - \omega_0^2 x \end{cases}. \tag{2}$$

As shown in Fig. 1, the limit cycle changes its shape from a quasi-circle curve into a jerky closed orbit (relaxation oscillation) with ε increasing. In this paper, the coefficient ε is fixed at 0.1 for satisfying the need of CPG-based locomotion controller design in Section III.

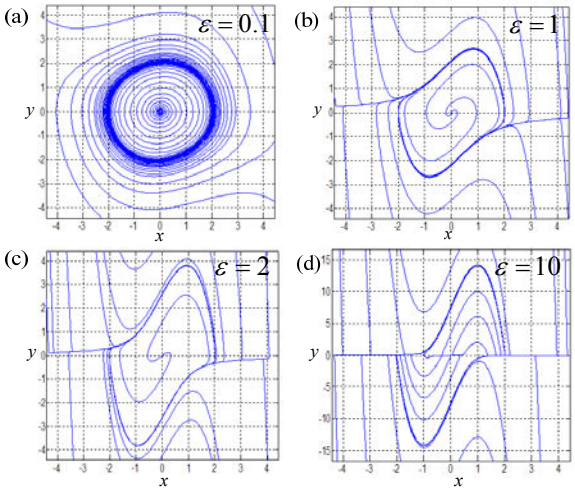

Fig. 1. Limit cycles of VDP model on phase plane with varied coefficient ε. Model parameter set: b =1 and ω_0 =1.

B. Perturbation Solution Based on MMS

The limit cycle generated by VDP model is globally stable on the phase plane, which is extremely advantageous to depict the rhythmic output of CPG network. To gain a deeper insight into the relationship between the periodic oscillation and model parameters, the analytical solution of VDP model has been derived based on perturbation theory. This will suffice for regulating the stable output of neuron model of CPG network. Herein we apply Method of Multiple Scales (MMS [20] to obtain the approximate analytical solution.

Let ξ and η be two time scales provided that ε is a sufficient small parameter. And then we change the independent variable from original system (1) from t to ξ and η as below

$$\begin{cases} \xi = \varepsilon t \\ \eta = (1 + \varepsilon^2\omega_2 + \varepsilon^3\omega_3 + \cdots \varepsilon^M\omega_M)t \end{cases}, \tag{3}$$

where ω_i is the undetermined frequency. Using the chain rule, we get

$$\begin{cases} \dfrac{d}{dt} = \varepsilon\dfrac{\partial}{\partial\xi} + (1 + \varepsilon^2\omega_2 + \varepsilon^3\omega_3 + \cdots + \varepsilon^M\omega_M)\dfrac{\partial}{\partial\eta} \\ \dfrac{d^2}{dt^2} = \varepsilon^2\dfrac{\partial^2}{\partial\xi^2} + 2\varepsilon(1 + \varepsilon^2\omega_2 + \varepsilon^3\omega_3 + \cdots + \varepsilon^M\omega_M)\dfrac{\partial^2}{\partial\eta\partial\xi} \\ \qquad + (1 + \varepsilon^2\omega_2 + \varepsilon^3\omega_3 + \cdots + \varepsilon^M\omega_M)^2\dfrac{\partial^2}{\partial\eta^2} \end{cases}. \tag{4}$$

We seek a uniform approximate solution to (1) under the new time scale (3) which can be expressed as

$$x = x_0(\xi,\eta) + \varepsilon x_1(\xi,\eta) + \varepsilon^2 x_2(\xi,\eta) + \cdots \quad . \tag{5}$$

Substituting (5) into (1) and equating each term of the coefficient of ε, we have

$$\varepsilon^0: \quad \frac{\partial^2 x_0}{\partial\eta^2} + \omega_0{}^2 x_0 = 0 \tag{6}$$

$$\varepsilon^1: \quad \frac{\partial^2 x_1}{\partial\eta^2} + \omega_0{}^2 x_1 = -2\frac{\partial^2 x_0}{\partial\xi\partial\eta} + (1 - bx_0{}^2)\frac{\partial x_0}{\partial\eta} \tag{7}$$

The general solution of (6) can be derived as

$$x_0 = a(\xi)\cos(\omega_0\eta + \varphi_0) \tag{8}$$

Substituting (8) into (7) and obtain

$$\frac{\partial^2 x_1}{\partial\eta^2} + \omega_0{}^2 x_1 = (2\frac{da}{d\xi} - a + \frac{ba^3}{4})\sin(\omega_0\eta + \varphi_0) + \frac{ba^3}{4}\sin 3(\omega_0\eta + \varphi_0) \tag{9}$$

Eliminate the secular term of $\sin(\omega_0\eta+\varphi_0)$, $a(\xi)$ can be determined as

$$a = \frac{2}{\sqrt{b + (\frac{4}{a_0^2} - b)e^{-\varepsilon t}}} \tag{10}$$

Note that the second time scale η contains $o(\varepsilon^2)$ and higher terms. Here we restrict the approximate solution within the first-order expansion of ε to reduce the complexity of algebra expression. Given the initial conditions of the original system (1), the approximation of VDP can be expressed as

$$x = \frac{2}{\sqrt{b + (\frac{4}{a_0^2} - b)e^{-\varepsilon t}}}\cos(\omega_0 t + \varphi_0). \tag{11}$$

C. Parameter Tuning

Since the analytical approximation of VDP model has been derived, the limit cycle of system (1) can be easily obtained as $t \to \infty$. Consequently we have

$$\begin{cases} x_\infty(t) = \dfrac{2}{\sqrt{b}}\cos(\omega_0 t + \varphi_0) \\ y_\infty(t) = -\dfrac{2\omega_0}{\sqrt{b}}\sin(\omega_0 t + \varphi_0) \end{cases} \tag{12}$$

Obviously, the amplitude and frequency of the limit cycle generated by VDP model can be specified by b and ω_0. The stable output of VDP model should be convenient for further gait generator and single-leg controller design. Meanwhile the motor capability and hardware capacity of the hexapod robot prototype built in our lab should also be considered accordingly. To this end, we set these two parameters as

$$\begin{cases} \dfrac{2}{\sqrt{b}} = 1 \\ \dfrac{2\pi}{\omega_0} = 5 \end{cases} \Rightarrow \begin{cases} b = 4 \\ \omega_0 = 0.4\pi \end{cases}. \tag{13}$$

Consequently, the CPG output is restricted on the unit cycle and the nominal vibration period is 5s.

III. CPG-BASED LOCOMOTION CONTROL FOR HEXAPOD ROBOT

The CPG-based locomotion control draws and recast the neurobiological findings via a mechanism that in essence is constructing a group or network of nonlinear oscillators to exhibit abundant outputs of CPG neurons in different phases and amplitudes. In this section, we address the problem of hexapod locomotion control from perspective of synchronization of coupled nonlinear oscillators. The locomotion control of hexapod robot can be divided into two levels. The first level focuses on adjusting the phase order of leg movement, and we propose a VDP-based gait generator to perform stable phase-locked signals exhibiting various gaits. The second level is to coordinate the joint motions of single leg in feasible working space. We fulfill this target by virtue of a three-coupled CPG network to produce adjustable trajectories without conflict with mechanical constraint. The whole body control architecture will be further established with combination of the gait generator and single-leg controller to achieve multiple gaits and gait transition for hexapod walking robot.

A. Gait Generator

Traditionally, the output of CPG unit is non-dimensional signal so that the relationship between the rhythmic signal of the CPG unit and locomotion of the hexapod robot should be established. As illustrated in Fig. 2, each unit contains two state variables are defined in (2) while the periodic output of the unit is mapped into the leg movement of the hexapod robot in one step cycle. The rising part of the signal denotes the swing phase while the descending part denotes the stance phase. Based on the previous analytical results in Section II-B, the phase order and duty factor of the hexapod gait could be accurately modulated via adjusting the parameters in VDP model to satisfy the locomotion requirements on different circumstances.

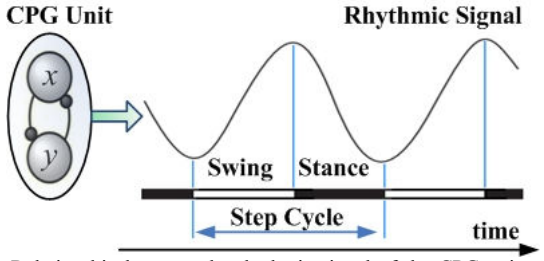

Fig. 2. Relationship between the rhythmic signal of the CPG unit and gait decomposition in one step cycle.

Since the connection between the CPG unit and gait parameters is specified, this unit could be extended to coupled-CPGs in order to construct a network. The configuration of CPG network as the gait generator for hexapod robot is shown in Fig. 3. Particularly, we develop the CPG network in ring shape considering that each CPG unit is identical in mathematics and interacts with only one adjacent neuron.

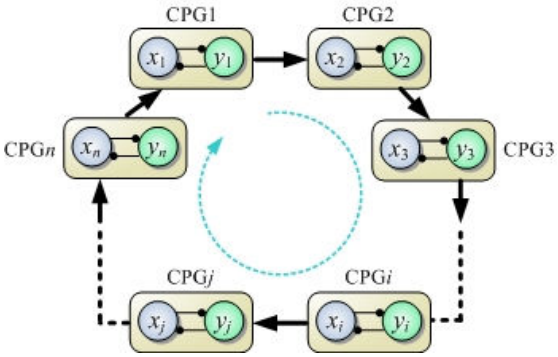

Fig. 3. The schematic of the gait generator with CPG units in ring shape

In this way, the problem of gait regulation of hexapod robot can be transformed into the synchronization and phase-locked problem of dynamic systems to handle. Without loss of generality, it is assumed that the neuron models of CPG network are identical from the ith unit to nth. The design of the gait generator obeys the following rules:

(1) The two neighbor neurons CPGi and CPGj produce periodic signals with identical amplitude and frequency.

(2) The phase difference of CPGi and CPGj should be locked at θ_i, and could be preciously shifted according to different gait types.

(3) The phase difference θ_i should be contained in the CPG network as an explicit expression.

Rule 1 restricts the boundary of rhythmic signals of the CPG neurons because the limit cycle of VDP model has been fixed at unit cycle on the phase plane in Section II-C. Rule 2 guarantees the stability of phase-locked within CPG units such that the stable gait can be attained. Moreover, the ability of phase difference shift is the essence of gait transition for hexapod robot. Finally Rule 3 is formulated to reduce the computing complexity of CPG network.

Now we start to design the CPG-based gait generator. Given the ith CPG unit as below

$$\begin{cases} \dot{x}_i = y_i \\ \dot{y}_i = \varepsilon(1 - bx_i^2)y_i - \omega_0^2 x_i \end{cases}. \tag{14}$$

The corresponding limit cycle can be derived through (12) as

$$\begin{cases} x_i^{\infty} = \dfrac{2}{\sqrt{b}}\cos(\omega_0 t + \varphi_{0i}) \\ y_i^{\infty} = -\dfrac{2\omega_0}{\sqrt{b}}\sin(\omega_0 t + \varphi_{0i}) \end{cases}. \tag{15}$$

According to Rule 2, the limit cycle of the *j*th CPG unit is written as

$$\begin{cases} x_j^{\infty} = \dfrac{2}{\sqrt{b}}\cos(\omega_0 t + \varphi_{0i} + \theta_i) \\ y_j^{\infty} = -\dfrac{2\omega_0}{\sqrt{b}}\sin(\omega_0 t + \varphi_{0i} + \theta_i) \end{cases}. \tag{16}$$

Comparing (15) to (16), we can further derive

$$\begin{pmatrix} x_j^{\infty} \\ y_j^{\infty} \end{pmatrix} = \mathbf{R}_{\theta_i} \begin{pmatrix} x_i^{\infty} \\ y_i^{\infty} \end{pmatrix}, \tag{17}$$

where $\mathbf{R}_{0i}$ is defined as the phase transition matrix from CPG*i* to CPG*j*, and R_{0i} can be written as

$$\mathbf{R}_{\theta_i} \triangleq \begin{pmatrix} \cos\theta_i & -\sin\theta_i \\ \sin\theta_i & \cos\theta_i \end{pmatrix}. \tag{18}$$

Up to now the integrated CPG network in ring depicted in Fig. 3 can be constructed as below

$$\begin{cases} \dot{\tilde{x}}_1 = f(\tilde{x}_1) + (\mathbf{R}_{\theta_1}\tilde{x}_2 - \tilde{x}_1) \\ \dot{\tilde{x}}_2 = f(\tilde{x}_2) + (\mathbf{R}_{\theta_2}\tilde{x}_3 - \tilde{x}_2) \\ \vdots \quad\quad \vdots \quad\quad\quad \vdots \\ \dot{\tilde{x}}_n = f(\tilde{x}_n) + (\mathbf{R}_{\theta_n}\tilde{x}_1 - \tilde{x}_n) \end{cases} \tag{19}$$

where $\tilde{x}_i$ is the state variable of single CPG unit in (14) and $\tilde{x}_i = [x_i, y_i]^T$. $f(\tilde{x}_i)$ is the VDP model in state-space, which is expressed as

$$f(\tilde{x}_i) = \begin{pmatrix} y_i \\ \varepsilon(1 - bx_i^2)y_i - \omega_0^2 x_i \end{pmatrix}. \tag{20}$$

The global synchronization and stability of network (19) is guaranteed via nonlinear contraction theory proposed by Lohmiller and Slotine et al [21] (see [22] for detail proofs). Furthermore, the global synchronization and phase-locked of the CPG network reveal that for a given target gait, the outputs of coupled oscillators will converge into the corresponding phase relationship regardless of the initial conditions of the differential system.

Particularly, the gait generator for the hexapod robot is acquired as the number of neurons $n = 6$. Fig. 4 illustrates the numerical simulations on the tripod and tetrapod gait generation based on the network proposed in (19). The detail information of the phase difference used to produce these two gaits is listed in Table I. Note that the tripod gait consists of two pairs of three legs in phase: {L1,R2,L3} and {R1,L2,R3} while the tetrapod has three: {L1,R2}, {L2,R3} and {L3,R1}. The wave gait has six: {L1},{R3},{L3},{R2},{L2},{R1} in order. Theoretically, each group shares the identical period of the ordinary gait. In this way, it is clear to reveal that the tripod, tetrapod and wave gait respectively has 2, 3 and 6 time-ticks.

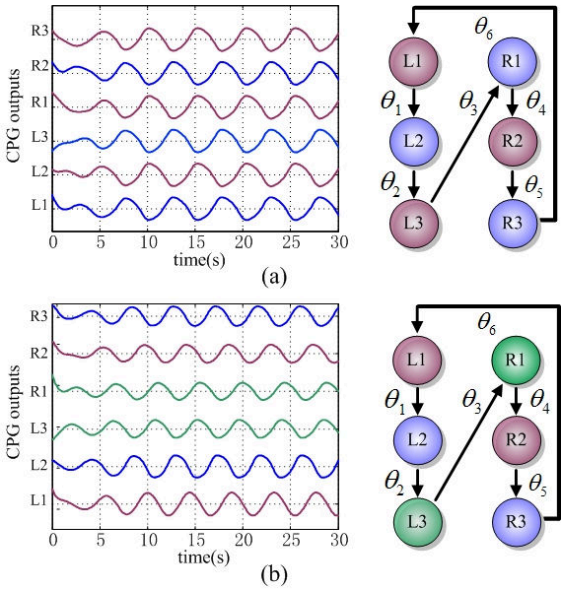

Fig. 4. The CPG-based gait generator for the hexapod robot in two typical gaits. (a) Tripod gait: the CPG outputs (left) and schematic of network in ring (right). (b) Tetrapod gait: the CPG outputs (left) and schematic of network in ring (right). The symbol L and R represent the leg on left and right side of body, respectively.

TABLE I. PHASE DIFFERENCE IN TWO GAITS

Gait	Phase Difference					
	θ_1	θ_2	θ_3	θ_4	θ_5	θ_6
Tripod	π					
Tetrapod	$2\pi/3$	$2\pi/3$	0	$2\pi/3$	$2\pi/3$	$4\pi/3$
Wave	$2\pi/3$					

Another significant phenomenon during gait generation is called gait transition which means the current gait could shift into another gait type in finite time. Theoretically, generating stable gait from arbitrary initial conditions of neurons shares the uniform fundamental with gait transition, which is the global synchronization of network. The gait transition can be understood as the coupled CPG network has the ability to recover from the initial condition "out of phase" at the transition time instant to the desired state "in phase" of the target gait. The numerical results of the tripod-tetrapod gait transition are shown in Fig. 5. The transition time is set at different time instant. The CPG outputs rapidly converge into the desired phase-locked state for the tetrapod gait.

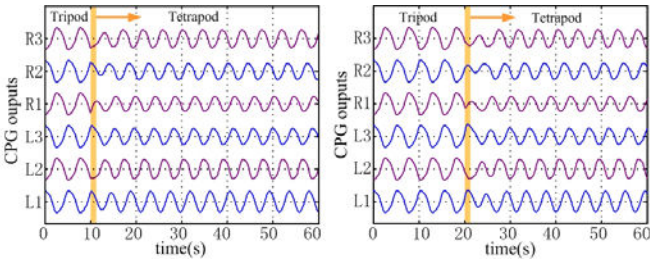

Fig. 5. The tripod-tetrapod gait transition at t =10s (left) and t =20s (right).

B. Single-leg Controller Design

As mentioned in Section II, the first level of the CPG-based locomotion control deals with the movement between legs has been accomplished in the gait generator design. In this section, we focus on the coordination of the multiple DoFs motions of the single leg for the hexapod robot.

Similarly, we choose the VDP model as the basic neuron composer to build a single leg controller as shown in Fig. 6.

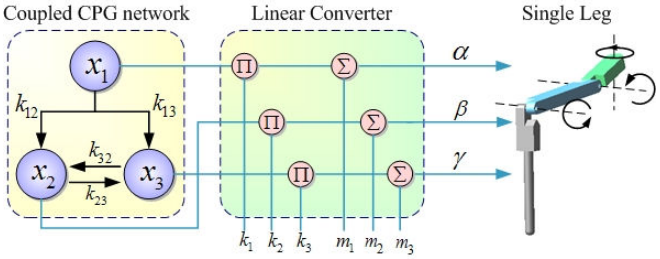

Fig. 6. The single leg controller for the hexapod robot. α, β and γ denote the body-coax, coax-femur and femur-tibia joint of the leg, respectively.

The controller is divided into two parts, namely, a coupled CPG network with three oscillators and a linear converter. This network operates as a phase modulator and produces three phase-locked rhythmic waves with adjustable frequencies, the mathematical description of which is given by

$$\begin{cases} \ddot{x}_1 + \varepsilon_1(b_1 x_1^2 - 1)\dot{x}_1 + \omega_1^2 x_1 = 0 \\ \ddot{x}_2 + \varepsilon_2(b_2 x_2^2 - 1)\dot{x}_2 + \omega_2^2 x_2 = k_{12}\dot{x}_1 x_1 + k_{32}(\dot{x}_2 - \dot{x}_3) \\ \ddot{x}_3 + \varepsilon_3(b_3 x_3^2 - 1)\dot{x}_3 + \omega_3^2 x_3 = k_{13}\dot{x}_1 x_1 + k_{23}(\dot{x}_3 - \dot{x}_2) \end{cases}, \quad (21)$$

where x_i is the state of the neuron. ω_i is the adjustable frequency according to different gait requirements. kij is the mutual connections. Here x_1 acts as the master neuron and x_2, x_3 acts as the slave neurons to receive the orders from x_1. The coupled terms in the 2nd and 3rd equations of (21) are designed to synchronize two slave neurons.

The linear convertor operates as an amplitude modulator. It transfers the CPG outputs in (21) from the unit cycle into the joint space according to the kinematics of the robot via

$$\begin{cases} \alpha = k_1 x_1 + m_1 \\ \beta = k_2 x_2 + m_2 \\ \gamma = k_3 x_3 + m_3 \end{cases}, \quad (22)$$

where k_i and m_i are the amplified coefficient and bias. After parameter tuning, the proposed single-leg controller products a series of stable limit cycles for the joints coordination in stance and swing phase as Fig. 7 shows.

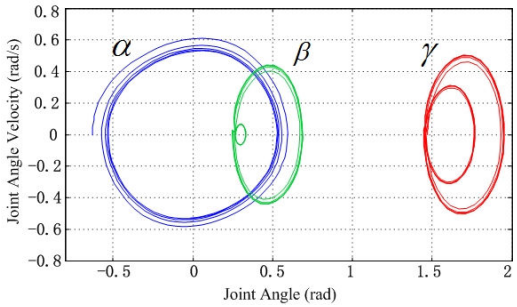

Fig. 7. The limit cycles on the phase plane of single leg joints. For β (green) and γ (red) joints, the inner closed orbit represents the trajectory in stance while the outer represents the swing phase.

C. Whole Body Control Architecture

Combining the gait generator and single-leg controller, we propose the whole body hierarchical control architecture as shown in Fig. 8. The gait generator with the CPG network in ring described above is located at the top level. The various gait types as well as gait transition is realized by directly setting the corresponding phase differences between the CPG units. Combined with the Finite State Machine (FSM), the single-leg controller constitutes the lower level. The FSM is introduced here to schedule the assignment of leg movement during walking. The FSM extends the traditional gait phases into three states: swing, stance as well as hold state which is added to describe the situation that the legs in stance hold their position to wait the untouched legs when local reflex behavior is trigged or other emergence occurs (these cases are beyond the scope of this work, so not discussed in this paper). The single-leg controller regulates the desired trajectories of joints with specified phase and amplitude. Additionally, the PD control is implemented at each joint to tracking the desired motion generated by the linear converter.

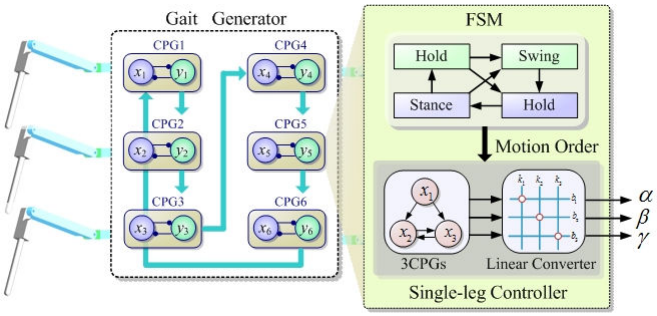

Fig. 8. Whole body control architecture for the hexapod robot

IV. Simulation and Experiment

The effectiveness of the presented algorithm has been verified via computer simulation and physical experiment. The simulation is carried out by MSC.ADAMS™ to establish a virtual robot-ground platform. The motion command issued by the whole body controller is real-time calculated in MATLAB (R2008b, The MathWorks Inc., Natick, MA, USA). The fourth order Runge-Kutta variable-step method (ode45) is implemented to solve the dynamics of the CPG network. The maximum time-step size of 10^{-3} together with relative and absolute tolerance $\leq 10^{-8}$ is set to guarantee the computational accuracy. The real physical robot experiment has been implemented with a hexapod robot prototype to test the gait generation and GAIT TRANSITION algorithm.

A. Hexapod Robot Prototype

The hexapod robot prototype designed and manufactured in our lab is shown in Fig. 9. The six identical legs with three rotary joints are equipped on the aluminum body. The elastic element with spring is installed at each foot to reduce the impact during touchdown which is detected by a contact sensitive cell with binary feedback mounted at the toe of each foot.

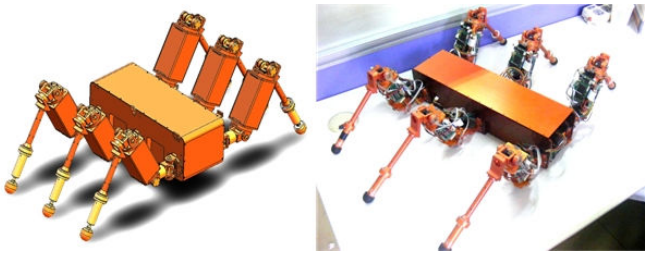

Fig. 9. The hexapod robot: CAD model (left) and physical prototype (right)

The electrical system includes three layers: the top layer contains the ARM 9 microprocessor (Samsung Inc. S3C2440) to take charge of task scheduling and wireless communication with PC. The FPGA-based on-chip system (ALTERA, CycloneII) is employed to regulate the joint movement. The master/slave bus with star structure is implemented to send motion orders from the CPG network to the hardware driver. The lower layer deals with the encoder signals sampling, contact detection and RS485-PC connection as well as the closed-loop control of brushless DC motors (Maxon, EC32).

B. *Simulation Results*

The gait generation and transition simulation are performed to validate the algorithm proposed above. The decomposition diagram of the entire locomotion is recorded as Fig. 10 shows. The walking test begins with the tripod gait and the following gait types are in order: tetrapod→wave→tripod. Three gait transition commands are issued in sequence. The robot just takes several steps from the current gait to the desired gait and maintains this stable gait type afterwards. Owing to the special phase modulation of the gait generator, meanwhile considering the static stability of the hexapod robot walking, the robot has to perform gait transition just after all legs touchdown, which indicates that the actual transition moment is sort of "time-delay" compared to the gait transition order is issued.

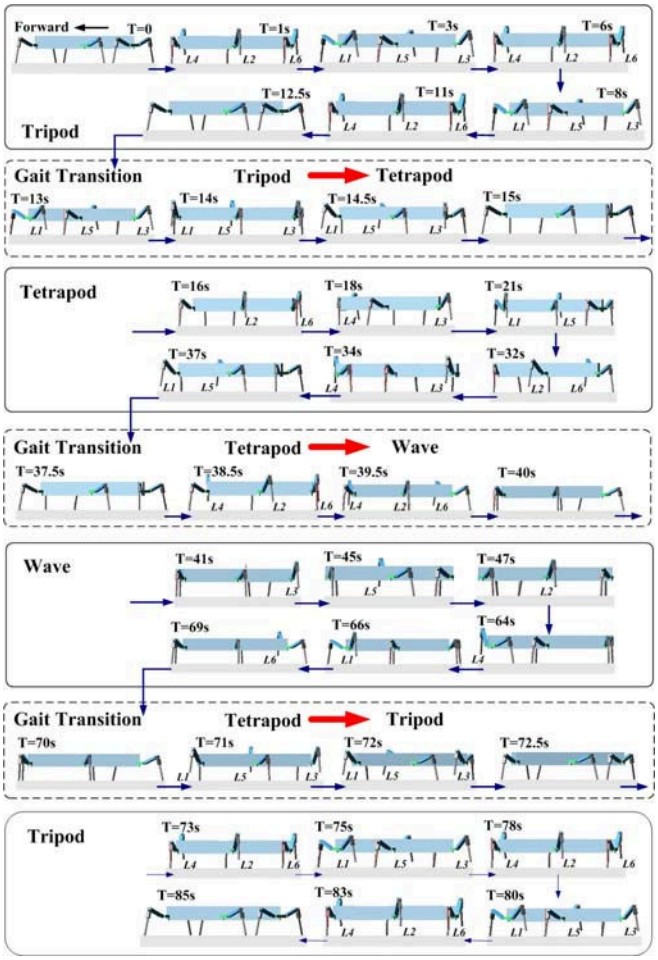

Fig. 10. The decomposition diagram of the gait transition simulation.

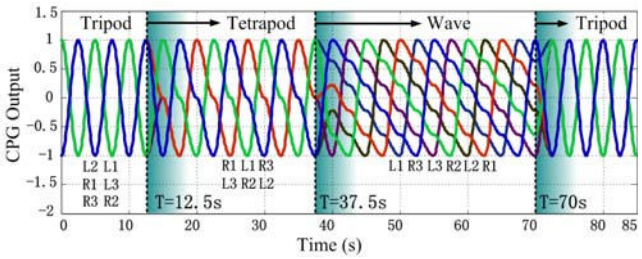

Fig. 11. The CPG output in the gait transition simulation.

Fig. 11 shows the corresponding CPG output of the gait generator after the FSM processing. The boundary of the CPG outputs are scaled into the region $[-1, 1]$ due to the parameter tuning in with $b = 4$ and $\omega_0 = 0.4\pi$. Here the wave gait represents the six legs of the hexapod robot start their movement in such order: L1→R3→L3→R2→L2→R1 (totally 6 time-ticks). It is clearly to observe that the gait generator could produce the expected gait with specified phase relationship. The gait transitions among tripod→tetrapod→wave→tripod are accomplished in no longer than 1 time-tick (roughly 2.5s) to converge into the required gait. Also note that the rhythmic curve in tetrapod gait and wave gait looks jerky because the rhythmic smooth signals produced by the gait generator have to be lengthened in the FSM so that the legs in different state (swing or stance) could synchronize with each other without break the kinematic constrains of the mechanical structure of the hexapod robot.

B. *Experiment Results*

The walking test is also implemented with the real physical hexapod robot described Section IV-A. The robot begins with

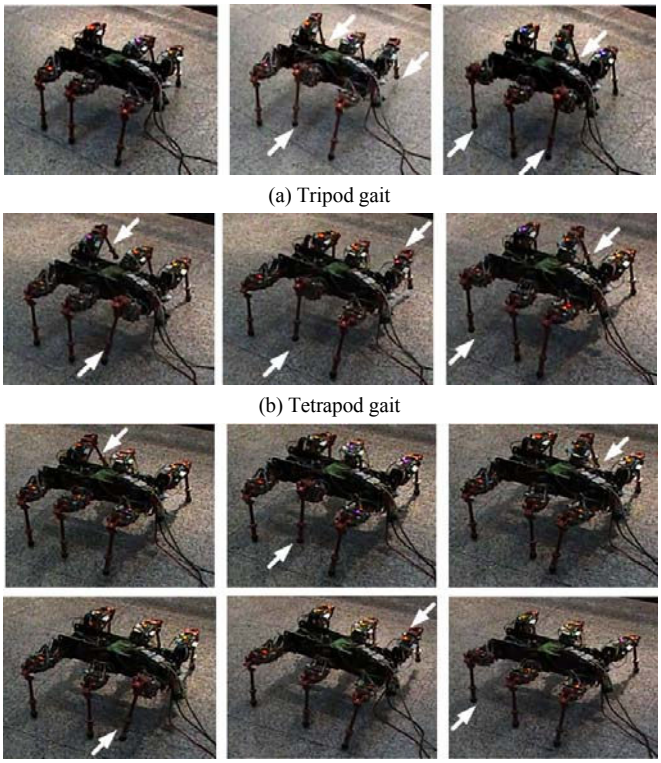

(a) Tripod gait

(b) Tetrapod gait

(c) Wave gait

Fig. 12. Snapshots of the hexapod robot during walking test. The leg in swing phase is marked with white arrow for clearance.

tripod gait and switches into tetrapod, wave and tripod gait in turn. Each gait sustains just two periods. The snapshots of the walking experiment are illustrated in Fig. 12 (the gait transition sections are omitted for brevity). The robot exhibits stable and various walking gait and undergoes smooth and rapid transition to each desired gait type, which is closely in agreement with the simulation results. In addition, the Center of Mass (CoM) motion of the robot is also recorded as shown in Fig. 13. The forward velocity of body displays a fluctuant character rather than constant value due to the output of the coupled nonlinear VDP oscillators in single-leg controller. The frequencies of both gait generator and single-leg controller are fixed at 0.4π. In this manner, tripod is the fastest gait type because it just needs two time-ticks to circulate whole legs movement while wave gait with six ticks is the slowest one as shown in Fig. 13.

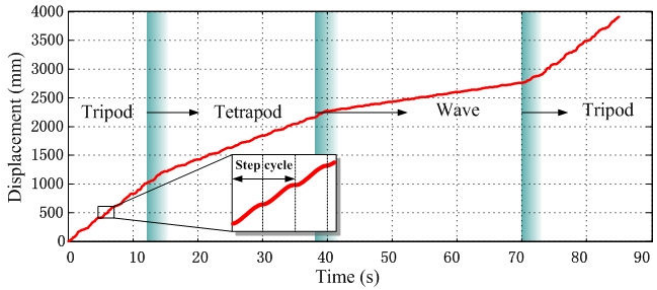

Fig. 13. Trajectory of the CoM motion during the walking test.

V. Conclusions and Discussion

In this paper, we presented a novel CPG-based locomotion control architecture for hexapod robot. With the help of perturbation technique, we could investigate the CPG systems with an analytical approach. The motion control of legged robot can be further divided into the phase modulation domain and amplitude regulation domain. The modified VDP model was introduced to establish the gait generator composed of CPG network in ring configuration to achieve various gait and gait transition. The single-leg controller with coupled CPG networks was developed to coordinate the joints motion. The validity of the proposed algorithm had been confirmed via the walking simulation and real physical robot experiment.

The proposed control framework sheds light on the methodology on CPG-based locomotion controller design for legged robot. Furthermore, the gait generator with VDP oscillator could be easily extended into cascaded form which is especially suitable to snakelike robot. Our future work will extend towards two directions. Foremost, the coupling of the CPG-based algorithm and the mechanical structure constraints of legged robot should be deeply investigated. Second, the more complicated dynamic behavior of the coupled CPG network should be merged into the limit cycle-based system to mimic the skillful local reflex behaviors of animals in unstructured environment.

References

[1] M. H. Raibert, *Legged Robots that Balance*. MIT Press, Cambridge, MA, 1986.

[2] R. Altendorfer, R. W. Longman, M. Buehler, "Rhex: A biologically inspired hexapod runner," *Autonomous Robots*, vol.11, pp. 207-213, 2001.

[3] V. Durr, J. Schmitz, H. Cruse, "Behaviour-based modeling of hexapod locomotion: linking biology and technical application," *Arthropod Structure & Development*, vol.33, pp. 237-250, 2004.

[4] H. Kimura, Y. Fukuoka, A. H. Cohen, "Adaptive dynamic walking of a quadruped robot on natural ground based on biological concepts," *International Journal of Robotics Research*, vol.26, pp.475-490, 2007.

[5] A. J. Ijspeert, A. Crespi, D. Ryczko, "From swimming to walking with a salamander robot driven by a spinal cord model" *Science*, vol.315, pp. 1416-1420, 2007.

[6] F. Delcomyn, "Neural basis for rhythmic behavior in animals," *Science*, vol.210, pp.492-498, 1980,

[7] I. Delvolvé, P. Branchereau, R. Dubuc, J.M. Cabelguen, "Fictive rhythmic motor patterns induced by NMDA in an in vitro brain stem-spinal cord preparation from an adult urodele," *Journal of Neurophysiology*, vol.82, pp.1074-1077, 1999.

[8] A. H. Cohen, P. Holmes, R. Rand, "The nature of coupling between segmented oscillations and the lamprey spinal generator for locomotion: A mathematical model," *Journal of Mathematical Biology*, vol.13, pp.345-369, 1982.

[9] K. Matsuoka, "Mechanisms of frequency and pattern control in the neural rhythm generators," *Biological Cybernetics*, vol.56, pp.345-353, 1987.

[10] G. Taga, "A model of the neuro-musculo-skeletal system for anticipatory adjustment of human locomotion during obstacle avoidance," *Biological Cybernetics*, vol.78, pp.9-17, 1998.

[11] R. Guanjiao, C. Weiahi, K. Christoph, et al, "Multiple chaotic central pattern generators for locomotion generation and leg damage compensation in a hexapod robot," *Proceedings of the IEEE International Conference on Intelligent Robots and Systems*, 2012, pp.2756-2761.

[12] A. Crespi, J. Ijspeert, "Online optimization of swimming and crawling in an amphibious snake robot," *IEEE Transactions on Robotics*, vol.24, pp.75-87, 2008.

[13] A. J. Ijspeert, A. Crespi, J. M. Cabelguen, "Simulation an robotics studies of salamander locomotion: Applying neurobiological principles to the control of locomotion in robots," *NeuroInformatics*, vol.3, pp.171-196, 2005.

[14] K. Inoue, S. Ma, C.Jin, "Neural oscillator network-based controller for meandering locomotion of snake-like robots," *Proceedings of the IEEE International Conference on Robotics and Automation*, 2004, pp.5064-5069.

[15] S. D. Prentice, A. E. Patla, D. A. Stacey, "Simple artificial neural network models can generate basic muscle activity patterns for human locomotion at different speeds," *Experimental Brain Research*, vol.123, pp. 474-480, 1998.

[16] M. Okada, K. Tatani, Y. Nakamura, "Polynomial design of the nonlinear dynamics for the brain-like information processing of whole body motion," *Proceedings of the IEEE International Conference on Robotics and Automation*, 2002, pp.1410-1415.

[17] A. Ijspeert, J. Hallam, D. Willshaw, "Evolving swimming controllers for a simulated lamprey with inspiration from neurobiology," *Adaptive Behavior*, vol.7, pp.151-172, 1999.

[18] R. D. Beer, J. C. Callagher, "Evolving dynamical neural networks for adaptive behavior," *Adaptive Behavior*, vol.1, pp.91-122, 1992.

[19] B. Van der Pol, "On relaxation-oscillations," *Philosophical Magazine*, vol.2, pp.978-992, 1927.

[20] A. H. Nayfeh, *Introduction to perturbation techniques*.CA: John Wiley & Sons, 1981.

[21] W. Hohmiller, J. J. Slotine, "On contraction analysis for nonlinear systems," *Automatica*, vol.34, pp.671-682, 1998.

[22] Q. C. Pham, J. J. Slotine, "Stable concurrent synchronization in dynamic system networks," *Neural Networks*, vol.20, pp.62-77, 2007.